

# Visualising active species in CO<sub>2</sub> electroreduction

Yu Yang<sup>1</sup>, Yaohui Shi<sup>2</sup>, Fengwang Li<sup>1\*</sup>

<sup>1</sup>School of Chemical and Biomolecular Engineering and ARC Centre of Excellence for Green Electrochemical Transformation of Carbon Dioxide, The University of Sydney, NSW 2006, Australia

<sup>2</sup>Hefei National Research Center for Physical Sciences at the Microscale, University of Science and Technology of China, Hefei, Anhui, 230026, P. R. China

\*Corresponding author. Email: [fengwang.li@sydney.edu.au](mailto:fengwang.li@sydney.edu.au)

## Abstract

Understanding the evolution of Cu-based catalysts during electrochemical CO<sub>2</sub> reduction (ECR) remains challenging. The study by Lim et al. in *Joule* devises an *operando* scanning transmission X-ray microscopy to investigate the dynamic phase transformations of Cu catalysts and reveals that Cu<sup>2+</sup> species play a crucial role in enhancing C–C coupling. The findings inform the authors an approach to dynamically redirect the oxidation state of Cu, achieving, as a result, higher selectivity and efficiency for ECR catalysis.

## Main

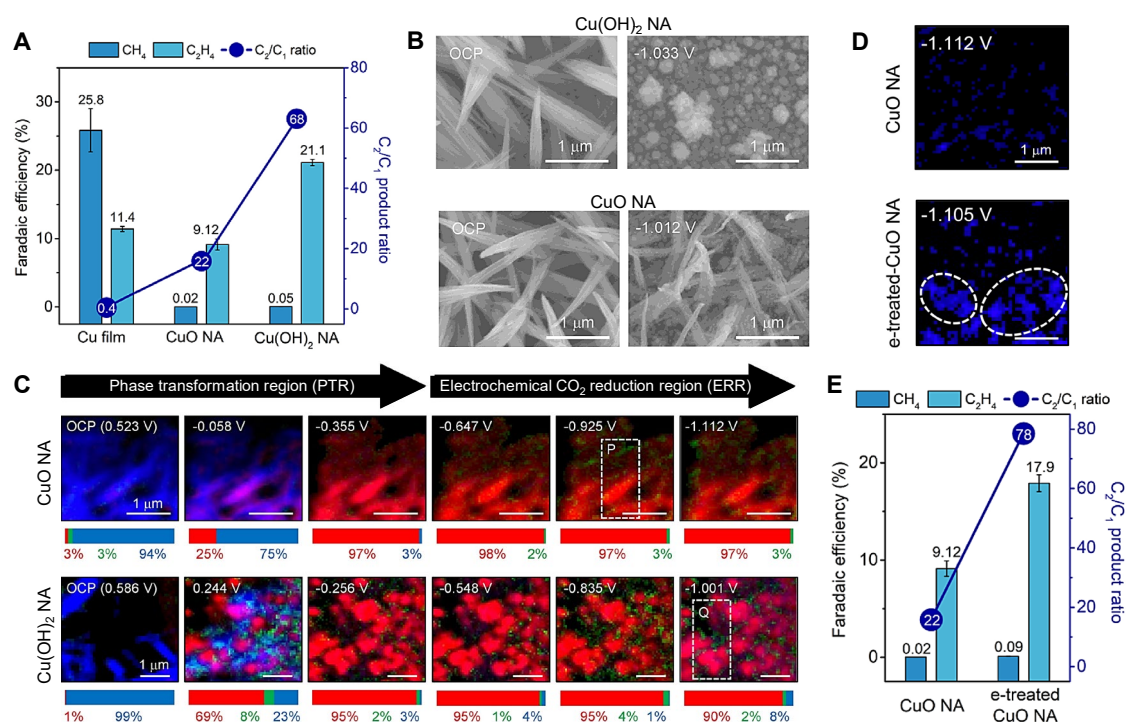
Electrochemical CO<sub>2</sub> reduction (ECR) is a promising technology for achieving net-zero carbon emissions and developing sustainable energy systems.<sup>1</sup> As one of the most promising non-precious metal catalysts for ECR, Cu-based catalysts can uniquely facilitate the formation of multi-carbon (C<sub>2+</sub>) products such as ethylene and ethanol.<sup>2</sup>

Previous studies demonstrated that the selectivity of Cu-based catalysts is correlated with the oxidation state of copper species.<sup>3</sup> During ECR, the dynamic evolution of Cu oxidation states, including Cu<sup>0</sup>, Cu<sup>+</sup>, and Cu<sup>2+</sup>, plays a critical role in modulating key reaction steps such as \*CO adsorption and C–C coupling.<sup>4</sup> For example, it has been suggested that partially oxidized Cu species (e.g., Cu<sup>+</sup>) enhance \*CO adsorption, thereby promoting C–C bond formation,<sup>5</sup> while metallic Cu (Cu<sup>0</sup>) facilitates the hydrogenation of adsorbed intermediates.<sup>6</sup> Nevertheless, there are few approaches to provide *in-situ*, real-time information on the dynamics of these diverse Cu states.

Traditional methods, such as bulk-averaged spectroscopy and *ex-situ* imaging, often fail to capture the real-time dynamics and spatial heterogeneity of Cu oxidation states at the nanoscale, limiting the comprehensive understanding of temporal evolution of Cu oxidation states during ECR and its relationship with the selectivity for C<sub>2+</sub> products.

Advanced techniques with high spatial and temporal resolution are essential. In this context, *operando* scanning transmission X-ray microscopy (STXM) has emerged as a promising tool, allowing the tracking of catalysts' real-time chemical and morphological changes with exceptionally high sensitivity.<sup>7</sup> By leveraging such innovative methods, Lim and co-workers reported their study in a recent *Joule* publication,<sup>8</sup> aiming to provide new insights into the dynamic phase evolution of Cu-based catalysts during ECR. The findings bridge the knowledge gap between catalyst structure and performance.

39 *Operando* STXM enabled the authors to track Cu-based catalysts' chemical and morphological  
 40 evolution in real-time, unveiling the critical role of oxidized copper species ( $\text{Cu}^+$  and  $\text{Cu}^{2+}$ ) in  
 41 enhancing catalytic activity. This advanced technique serves two crucial functions: (1) it  
 42 provides exceptional sensitivity for mapping various oxidation states of Cu, revealing a  
 43 significant correlation between the dynamic evolution of  $\text{Cu}^{2+}$  species on the metallic Cu  
 44 catalyst surface and enhanced C–C coupling; and (2) it proposes an electrochemical redirection  
 45 method of low- to high-activity catalysts by inducing  $\text{Cu}^{2+}$  phases.



46  
 47 **Figure 1.  $\text{CO}_2$  reduction performance and chemical composition images of the Cu-based**  
 48 **electrocatalysts during ECR**  
 49 (A) FE and  $\text{C}_2/\text{C}_1$  gaseous product ratio for CuO NA and  $\text{Cu}(\text{OH})_2$  NA at  $-1.0 \text{ V}_{\text{RHE}}$  in an H-type cell.  
 50 (B) SEM images of  $\text{Cu}(\text{OH})_2$  NA and CuO NA at specific potential (OCP and  $-1.0 \text{ V}_{\text{RHE}}$ ).  
 51 (C) Operando chemical composition mapping images of the CuO NA and  $\text{Cu}(\text{OH})_2$  NA electrocatalysts at the  
 52 phase transformation and electrochemical  $\text{CO}_2$  reduction regions.  
 53 (D)  $\text{Cu}^{2+}$  phase images of e-treated CuO NA and CuO NA at  $-1.0 \text{ V}_{\text{RHE}}$ . The intensity of the  $\text{Cu}^{2+}$  phase in the  
 54 images was magnified 25-fold after eliminating the noise level.  
 55 (E) Faradaic efficiencies and  $\text{C}_2/\text{C}_1$  product ratios of the CuO NA and e-treated CuO NA electrocatalysts at  
 56 approximately  $-1.0 \text{ V}_{\text{RHE}}$ .

57 To investigate the correlation between the morphological changes and evolution of the minor  
 58 oxidized species during ECR, the authors compared  $\text{Cu}(\text{OH})_2$  nano-needle array ( $\text{Cu}(\text{OH})_2$  NA)  
 59 with CuO NA, which has an identical  $\text{Cu}^{2+}$  oxidation state and similar shape to  $\text{Cu}(\text{OH})_2$  NA  
 60 as confirmed by Raman spectroscopy, X-ray absorption spectroscopy (XAS), and scanning  
 61 electron microscopy (SEM). When operating under ECR conditions in an H cell,  $\text{Cu}(\text{OH})_2$  NA  
 62 and CuO NA catalysts exhibit significant differences in product selectivity and post-reduction  
 63 morphology. The Faradaic efficiency (FE) ratios of the  $\text{C}_2/\text{C}_1$  products reveal that higher C–C  
 64 coupling selectivity was achieved on  $\text{Cu}(\text{OH})_2$  NA (67.8) than on CuO NA (22) (Figure 1A).  
 65 Meanwhile, SEM images showed that  $\text{Cu}(\text{OH})_2$  NA undergoes pronounced structural changes

66 while CuO NA retains its initial needle-like morphology (Figure 1B), suggesting that the  
67 evolution in Cu(OH)<sub>2</sub> NA during ECR is crucial in promoting multi-carbon product formation.

68 To understand the mechanisms underlying these differences, the researchers first excluded the  
69 influence of electrochemical surface area (ECSA) and grain size, then employed *operando*  
70 STXM at the Cu L<sub>3</sub>-edge with a spatial resolution of 50–75 nm to investigate changes in the  
71 local Cu oxidation state and morphology simultaneously (Figure 1C). By tracking the  
72 distribution of copper oxidation states at the nanoscale, they revealed that Cu(OH)<sub>2</sub> NA forms  
73 Cu<sup>0</sup> nano-agglomerates surrounded by Cu<sup>+</sup> and Cu<sup>2+</sup> localized at the edges of the Cu<sup>0</sup> domains  
74 during ECR. In contrast, CuO NA showed minimal formation of Cu<sup>2+</sup> species, correlating with  
75 its reduced ability to facilitate C<sub>2</sub> production. These observations suggest that the presence and  
76 distribution of Cu<sup>2+</sup> species are critical factors in determining the selectivity and efficiency of  
77 copper-based catalysts for ECR.

78 The authors proposed that the observed Cu<sup>2+</sup> species in Cu(OH)<sub>2</sub> NA were thermodynamically  
79 stabilized by copper (II) carbonate hydroxide species (Cu<sup>2+</sup><sub>x</sub>(CO<sub>3</sub>)<sub>y</sub>(OH)<sub>z</sub>) that dynamically  
80 persisted under ECR, as demonstrated through long-term *operando* STXM test and  
81 complementary *in-situ* surface-enhanced Raman spectroscopy (SERS). Using  
82 Cu<sup>2+</sup><sub>x</sub>(CO<sub>3</sub>)<sub>y</sub>(OH)<sub>z</sub> as the model for Cu<sup>2+</sup>-containing phases, density functional theory (DFT)  
83 calculations reveal that Cu<sup>2+</sup> significantly lowers the energy barrier for \*CO dimerization, a  
84 key step in ethylene formation. Besides, Cu<sup>2+</sup> species can also stabilize carbonyl oxygen of  
85 \*COOH (or \*CO<sub>2</sub>), enhancing the local \*CO/CO<sub>2</sub> concentration near the cathode, potentially  
86 accelerating the C–C coupling activity.

87 Building on these insights, the researchers developed a method to enhance C<sub>2</sub> selectivity by  
88 introducing Cu<sup>2+</sup> species into the catalyst structure. This redirection process partially reduced  
89 CuO NA to Cu<sub>2</sub>O phase under negative potentials, followed by spontaneous re-oxidation at  
90 open-circuit potential (OCP). During this process, Cu<sup>+</sup> dissolves into the electrolyte as Cu<sup>2+</sup>  
91 ions, which re-deposit onto the catalyst surface, creating Cu<sup>2+</sup> motifs, denoted as e-treated CuO  
92 NA catalysts (Figure 1D). This approach significantly improved C<sub>2</sub> selectivity, with the  
93 modified CuO NA achieving nearly double the FE for ethylene compared to its unmodified  
94 counterpart (Figure 1E). This finding underscores the potential of dynamic phase engineering  
95 to optimize catalyst performance.

96 While this study provides promising insights into the spatiotemporal evolution of copper-based  
97 catalysts during ECR using *operando* STXM, limitations of the technique and mechanism  
98 studies warrant further improvement and exploration.

99 The STXM reactor employed in this study closely resembles an H-cell configuration, which  
100 inherently operates at low current densities due to high internal resistance and low CO<sub>2</sub>  
101 availability. However, the performance and structural evolution of ECR catalysts can vary  
102 substantially between different cells or current densities, due to the discrepancy in the local  
103 reaction environment, mass transport dynamics, and pH distribution.<sup>9</sup> Therefore, Cu-based  
104 catalysts' structural evolution and reaction mechanisms in flow cells and membrane electrode  
105 assembly (MEA) systems require further investigation, coupled with technical advancements  
106 in *operando* techniques to accommodate these configurations.

107 While this study demonstrates the important role of Cu<sup>2+</sup> in promoting C<sub>2</sub> selectivity, it also  
108 acknowledges that Cu<sup>2+</sup> is not the only active site for C<sub>2</sub> product formation. For example, C<sub>2</sub>

109 products can still be generated in ECR when  $\text{Cu}^{2+}$  species are absent, as observed in the CuO  
110 NA catalyst. The inherent heterogeneity of active sites in copper-based catalysts complicates  
111 the establishment of clear links between catalytic performance and structure. For instance,  
112 introducing  $\text{Cu}^{2+}$  at OCP has limited control over the amount of  $\text{Cu}^{2+}$  formed during ECR  
113 turnovers, making it challenging to determine the optimal concentration of  $\text{Cu}^{2+}$  for  $\text{C}_2$   
114 production. This limitation hampers the rational design of highly efficient catalysts based on  
115 the  $\text{Cu}^{2+}$ -induced mechanisms proposed in this study.

116 Despite limits existing in the techniques, this work provides new insights into the dynamic  
117 evolution of Cu-based catalysts during ECR, emphasizing the critical role of  $\text{Cu}^{2+}$  species in  
118 enhancing  $\text{C}_2$  selectivity. Using *operando* STXM, the researchers precisely tracked real-time  
119 morphological and compositional changes in copper catalysts with a  $\sim 50$  nm spatial resolution.  
120 The findings reveal that stabilising  $\text{Cu}^{2+}$  species by forming  $\text{Cu}^{2+x}(\text{CO}_3)_y(\text{OH})_z$  phases  
121 promotes C–C coupling and multi-carbon product formation by lowering the energy barrier for  
122  $\ast\text{CO}$  dimerization and enhancing the local  $\ast\text{CO}/\text{CO}_2$  concentration. Moreover, the study  
123 highlights the potential of dynamic phase engineering, demonstrating how the deliberate  
124 introduction and stabilization of  $\text{Cu}^{2+}$  motifs can transform low-activity catalysts into highly  
125 selective systems for ECR.

## 126 Acknowledgements

127 The authors acknowledge support from the ARC Centre of Excellence for Green  
128 Electrochemical Transformation of Carbon Dioxide (CE230100017), funded by the Australian  
129 Government.

## 130 Declaration of interests

131 The authors declare no competing interests.

## 132 References

- 133 1. Stephens, I.E.L., Chan, K., Bagger, A., Boettcher, S.W., Bonin, J., Boutin, E., Buckley, A.K.,  
134 Buonsanti, R., Cave, E.R., Chang, X., et al. (2022). 2022 roadmap on low temperature  
135 electrochemical  $\text{CO}_2$  reduction. *JPhys Energy* 4, 042003. [https://doi.org/10.1088/2515-](https://doi.org/10.1088/2515-7655/ac7823)  
136 [7655/ac7823](https://doi.org/10.1088/2515-7655/ac7823).
- 137 2. Yan, T., Chen, X., Kumari, L., Lin, J., Li, M., Fan, Q., Chi, H., Meyer, T.J., Zhang, S., and Ma,  
138 X. (2023). Multiscale  $\text{CO}_2$  electrocatalysis to  $\text{C}_{2+}$  products: Reaction mechanisms, catalyst  
139 design, and device fabrication. *Chem. Rev.* 123, 10530-10583.  
140 <https://doi.org/10.1021/acs.chemrev.2c00514>.
- 141 3. Wu, H., Huang, L., Timoshenko, J., Qi, K., Wang, W., Liu, J., Zhang, Y., Yang, S., Petit, E.,  
142 Flaud, V., et al. (2024). Selective and energy-efficient electrosynthesis of ethylene from  $\text{CO}_2$  by  
143 tuning the valence of Cu catalysts through aryl diazonium functionalization. *Nat. Energy* 9,  
144 422-433. <https://doi.org/10.1038/s41560-024-01461-6>.
- 145 4. Vavra, J., Ramona, G.P.L., Dattila, F., Kormányos, A., Priamushko, T., Albertini, P.P., Loiudice,  
146 A., Cherevko, S., Lopéz, N., and Buonsanti, R. (2024). Solution-based  $\text{Cu}^+$  transient species  
147 mediate the reconstruction of copper electrocatalysts for  $\text{CO}_2$  reduction. *Nat. Catal.* 7, 89-97.  
148 <https://doi.org/10.1038/s41929-023-01070-8>.
- 149 5. Zang, Y., Liu, T., Wei, P., Li, H., Wang, Q., Wang, G., and Bao, X. (2022). Selective  $\text{CO}_2$   
150 electroreduction to ethanol over a carbon-coated  $\text{CuO}_x$  catalyst. *Angew. Chem., Int. Ed.* 61,  
151 e202209629. <https://doi.org/10.1002/anie.202209629>.

- 152 6. Chang, C.-J., Hung, S.-F., Hsu, C.-S., Chen, H.-C., Lin, S.-C., Liao, Y.-F., and Chen, H.M.  
153 (2019). Quantitatively unraveling the redox shuttle of spontaneous oxidation/electroreduction  
154 of CuO<sub>x</sub> on silver nanowires using in situ x-ray absorption spectroscopy. *ACS Cent. Sci.* 5,  
155 1998-2009. <https://doi.org/10.1021/acscentsci.9b01142>.
- 156 7. Mefford, J.T., Akbashev, A.R., Kang, M., Bentley, C.L., Gent, W.E., Deng, H.D., Alsem, D.H.,  
157 Yu, Y.-S., Salmon, N.J., Shapiro, D.A., et al. (2021). Correlative operando microscopy of  
158 oxygen evolution electrocatalysts. *Nature* 593, 67-73. [https://doi.org/10.1038/s41586-021-](https://doi.org/10.1038/s41586-021-03454-x)  
159 [03454-x](https://doi.org/10.1038/s41586-021-03454-x).
- 160 8. Kim, J., Lee, S.Y., Kim, S.-J., Koo, B., Chung, J., Lee, D., Choi, S., Kim, J., Seo, S., Nam, C.,  
161 et al. (2024). Spatiotemporal active phase evolution for CO<sub>2</sub> electrocatalysis. *Joule*.  
162 <https://doi.org/10.1016/j.joule.2024.09.008>.
- 163 9. Choi, W., Chae, Y., Liu, E., Kim, D., Drisdell, W.S., Oh, H.-s., Koh, J.H., Lee, D.K., Lee, U.,  
164 and Won, D.H. (2024). Exploring the influence of cell configurations on Cu catalyst  
165 reconstruction during CO<sub>2</sub> electroreduction. *Nat. Commun.* 15. [https://doi.org/10.1038/s41467-](https://doi.org/10.1038/s41467-024-52692-w)  
166 [024-52692-w](https://doi.org/10.1038/s41467-024-52692-w).

167